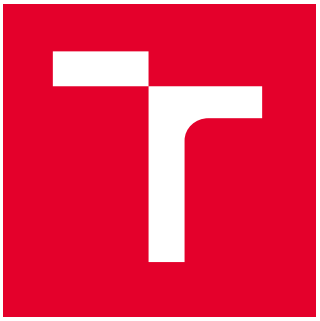

BRNO UNIVERSITY OF TECHNOLOGY

VYSOKÉ UČENÍ TECHNICKÉ V BRNĚ

FACULTY OF MECHANICAL ENGINEERING

FAKULTA STROJNÍHO INŽENÝRSTVÍ

INSTITUTE OF PHYSICAL ENGINEERING

ÚSTAV FYZIKÁLNÍHO INŽENÝRSTVÍ

LASER WITH NAROW SPECTRAL LINEWIDTH FOR METROLOGY OF LENGTH

JEDNOFREKVENČNÍ LASER S ÚZKOU SPEKTRÁLNÍ ČÁROU PRO METROLOGII DÉLEK

SUMMARY OF DOCTORAL THESIS

TEZE DIZERTAČNÍ PRÁCE

AUTHOR — **Ing. Minh Tuan Pham**

AUTOR PRÁCE

SUPERVISOR — **Ing. Ondřej Číp, Ph.D.**

ŠKOLITEL

BRNO 2022

Klíčová slova
Polovodičový laser s externím rezonátorem, optický rezonátor s vysokou jakostí, šířka spektrální čáry,stabilizace frekvence, kalciové hodiny, hodinový laser, fázový závěs, technika "transfer oscillator".

Keywords
External cavity diode laser, high-finesse optical cavity, spectral linewidth, frequency stabilisation, ion clocks, clock laser, phase lock loop, transfer oscillator technique.

Pham, M. T. *Jednofrekvenční laser s úzkou spektrální čárou pro metrologii délek* Brno: Vysoké učení technické v Brně, Fakulta strojního inženýrství, 2022, Vedoucí Ing. Ondřej Číp, Ph.D. ISBN (80-214- zbytek dolni redakce), ISSN 1213-4198.

Contents

Introduction and structure of the work

A *clock* is a device that uses the stable oscillation pattern as a reference (i.e. pendulum, quartz). An atomic clock is a laser whose frequency is stabilised relative to a narrow optical atomic transition. Thus the oscillator, in this case, is a trapped and isolated atom with a natural, very high oscillation rate. Thanks to this revolutionary idea and evolution of atomic frequency and time standards have taken a huge leap forward [1, 2, 3]. For nearly 100 years, the atomic frequency standard played a critical role in basic science and precision measurement. During this period, the increasing need for more precise timing and synchronisation for various applications, including navigation or test of fundamental physic, has demanded oscillators with higher frequencies and higher performance. The most recent clock can reach the stability or instability of 1.5 parts in a quintillion (1 followed by 18 zeros) in just a few thousand seconds [4].

This work closely relates to an optical atomic clock with a single $^{40}Ca^{+}$ ion. The infrastructure consisting of trapping apparatus, ultra-high vacuum chamber, laser requirement, and electronics was developed and fully built at the Institute of Scientific Instruments (ISI) in Brno. To be able to coherently transfer population between $4^2S_{1/2} \leftrightarrow 3^2D_{5/2}$ energy level, one needs a clock laser with an ultra-narrow spectral linewidth. This is a crucial part of the optical setup when realising the optical atomic clocks.

The main aim of this work is to design and build such a laser. The work focuses on implementing the best possible method for linewidth suppression available. The spectroscopy laser with suppressed linewidth to sub-Hz level gives us a tool for many experiments with trapped ions. Apart from the high-resolution spectroscopy on the ion forbidden transition for optical clock operations, it also allows us to individually manipulate the quantum state of ions. Thus, the clock laser is a gate for the information processing with cold ions going to quantum computers or quantum simulators.

Background of the research topic

This work has been done under the project on trapping and laser cooling of ions, which started in 2014. It is solved with the cooperation of two research groups. Our group from the Department of Coherence Optics of the Institute of Scientific Instruments CAS focuses on the infrastructure for the ion trapping and cooling, development of a Doppler cooling lasers, construction of the highly coherent laser source working at 729 nm and precision spectroscopy with ions stored in the radio frequency trap placed in the ultra-high vacuum chamber (both parts belong to my thesis).

The main research aim of our group is frequency metrology with the cold ion, which might be used for the realisation of an experimental optical atomic clocks. The second group is the team from the Department of Optics of Palacky University Olomouc. They focus mainly on quantum mechanics and information processing like quantum algorithms and multiparticle entanglement.

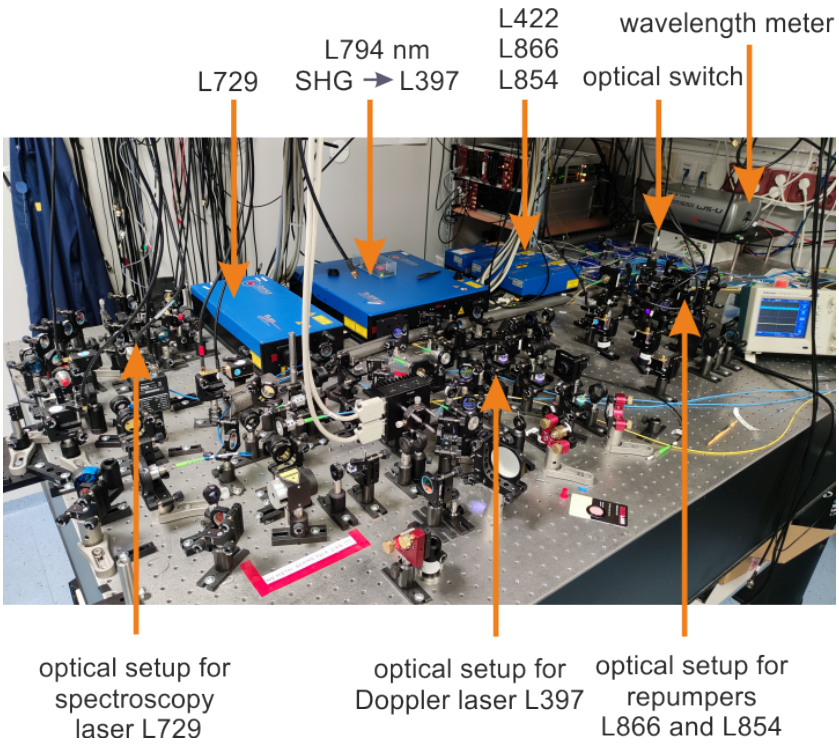

Figure 1: The overview over the optical table, where all the laser are prepared before being coupled and send into the chamber with the trapped ion. Each laser has several acousto-optic modulators placed in their path. They are used for frequency shifting, intensity stabilisation or serve in pulse sequence.

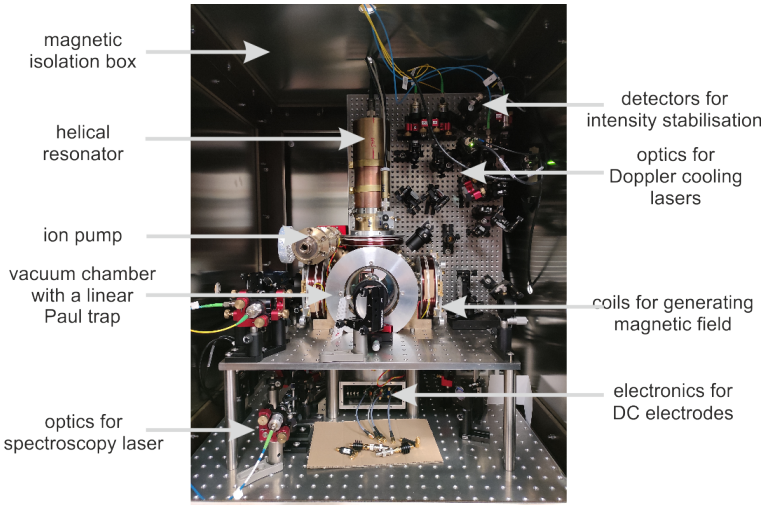

Figure 2: Ion trap apparatus with all necessary optics for Doppler cooling, sideband cooling and ion interrogation. The lasers are brought into setup via polarisation maintaining fibres. The main beam are prepared in terms of polarisation and position adjustment before entering the vacuum chamber. The ion fluorescence is collected by an collimating optic into an avalanche detector.

1. Optical atomic clock

1.1 Optical atomic clocks

Two primary approaches could be considered for building the clock as an optical frequency standard. One is a single ion isolated in a radio-frequency trap, and the second neutral atoms are trapped in a magneto-optical trap [5, 6]. Those systems, both placed in the ultra-high vacuum chambers, allow very high isolation of ions or atoms from external disturbances. Frequencies of narrow-band electronic transitions of those isolated ions are thus extremely stable references. Several of those systems have been already build over the years including $Al^{+}, Hg^{+/2+}, Hg, Sr, Sr^{+/2+}, In^{+/3+}, Mg, Ca, Ca^{V}, Yb^{+/2+/3+}$ and Yb [7, 8, 9].

Our laboratory aims to build an experimental optical clock with $^{40}Ca^{+}$ ion [10, 11, 12]. The great technological advantage why use Ca^{+}, is the availability of the wavelengths needed for ion excitation. They can be easily achieved with relatively well available laser diodes that allow large tuning over the frequencies see Subsec. 1.2.

By applying the radio frequency (RF) of 29.8 MHz and power of 4W to the trap electrodes and setting the mean tips voltage to 1200V, we achieve typical secular frequencies $\omega_r/2\pi = 2.7$ MHz in the radial and $\omega_a/2\pi = 1.1$ MHz in the axial direction. The single Ca^{+} ions are loaded into a trap by photo-ionising a beam of neutral calcium atoms. Everything enclosed by an ultrahigh vacuum $< 10^{-11}$ mbar [13], sufficient isolation from the environment perturbation. The trap apparatus is then situated inside a passive magnetic shield box to suppress the magnetic perturbation during the experiment [14, 15, 16, 17]. In the trap, we can hold either one single ion or an enormous Coulomb crystal consisting of tens of thousands of ions.

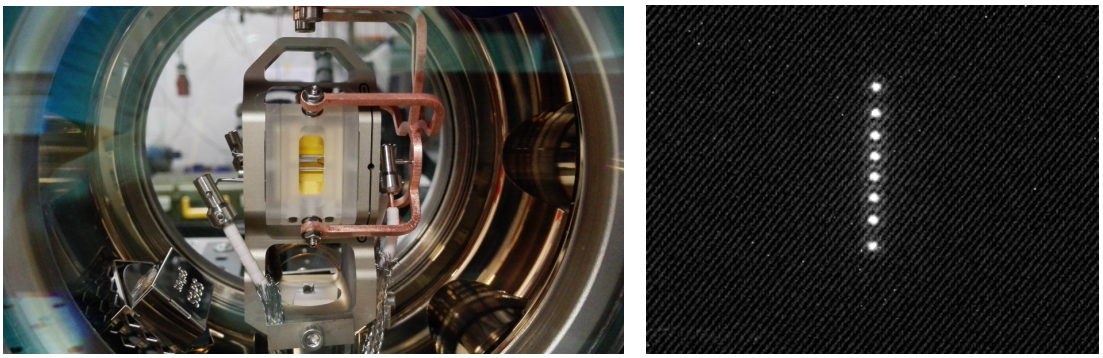

(a) (b)

Figure 1.1: A detailed view of the linear Paul trap with gold plated electrodes (a). A fluorescence from the Coulomb crystal made of 8 Ca ions. Ions are trapped and cooled to a temperature near absolute zero by interrogating with cooling lasers (b).

1.2 Laser-ion interactions

Level scheme of $^{40}Ca^{+}$

Natural calcium is a mixture of the 5 isotopes (^{40}Ca,^{42}Ca,^{43}Ca,^{44}Ca and ^{46}Ca). The most common isotope of the calcium is ^{40}Ca, which comprises 96,9% of all-natural calcium. It is the heaviest stable nuclide with equal proton and neutron numbers. Implementing the Calcium isotope as a stable reference has many advantages. Foremost all the relevant transitions are accessible by a solid-state laser source. The Fir. 1.2 shows the five lowest energy level.

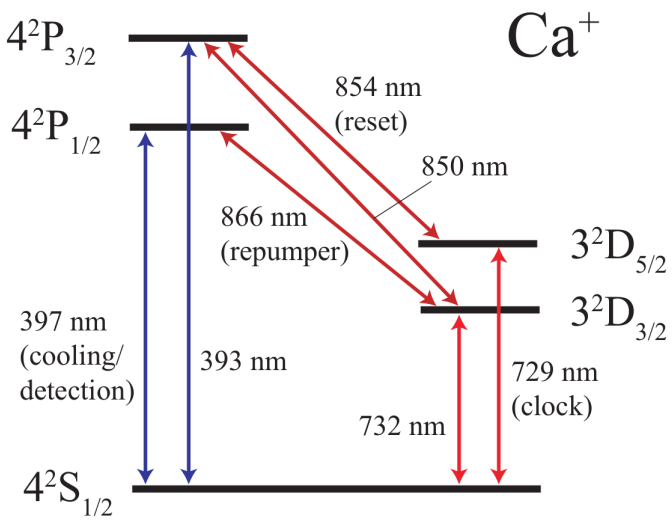

Figure 1.2: Level scheme of $^{40}Ca^{+}$. The $S \leftrightarrow P$ transition is used for Doppler cooling, while the $S \leftrightarrow D$ transition is used for quantum operations.

The Electric quadrupole transition of $^{40}Ca^{+}$

Compared to a dipole allowed transition which typically decay on ns [18], The $4^2S \leftrightarrow 3^2D$ transitions are the dipole-forbidden transitions with rather long lifetime (> 1 s). The natural linewidth of the transition is an inverse of the lifetime. Thus the linewidth of the transition is 1 Hz approx and less. This makes those transitions an ideal candidates for precision spectroscopy and optical atomic clock.

The $^{40}Ca^{+}$ clock transition is driven by a laser working on wavelength 729 nm. If the ion is placed inside a static magnetic field of a few Gauss, the Zeeman effect induced by this field defining by the quantization axis and by the electric quadrupole shift splits the $4^2S_{1/2} \leftrightarrow 3^2D_{5/2}$ into ten components. There are possible six transitions available for absolute frequency measurement i.e. the clock laser is locked to the $S - D$ transition.

2. Spectroscopy laser

The spectroscopy laser, also called a clock laser, is chosen for the excitation of a transition between two narrow fine energy levels of an atom. As was already mentioned in Chap. 1, our research group selected $^{40}Ca^{+}$ as a qubit for our experiments. The chosen transition is the electronic quadrupole from $S_{1/2}$ to $D_{5/2}$ level. The corresponding laser wavelength needed to probe this transition is around 729 nm. The natural linewidth of this transition is given by the inverse of the lifetime. So the long lifetime of the states makes these transitions an ideal candidate for high-resolution spectroscopy [19] and for the realisation of an optical clock. For these purposes, the interrogation clock laser must have the spectral line width at the Hz or sub-Hz level.

The operation of the spectroscopy laser are:

- high-resolution spectroscopy of narrow transitions,
- resolved sideband cooling of the ion motion,
- detection of the state by electron shelving technique,
- measuring the heating rate of the system using the Rabi spectroscopy,
- measuring the qubit coherence using the Ramsey spectroscopy,
- measuring the stability of the $^{40}Ca^{+}$ clock.

2.1 External cavity diode laser

In general, there are available three kinds of lasers that work at the wavelength range of 729 nm. They are dye lasers, optically pumped solid-state lasers and semiconductor lasers. A very promising was the optically pumped Ti:Sapphire solid-state laser, which can reach the linewidth at about 25 kHz [20]. Furthermore, it has a very low noise floor close to the emission line. Nevertheless, the laser needs external optical pumping, which carries an additional laser source and thus a requirement for the optical table space. Dye lasers also have external optical pumping, but they also have a poisonous operation due to the toxicity of dye's active matter [21, 22].

The semiconductor lasers come with a compact size, wide tuning range, and high power. A special types of diode laser are external-cavity diode lasers (ECDL) [23]. Compared with a standard laser diode, the ECDL has a longer cavity that increases the damping time of the intracavity light and thus allows for lower phase noise and a smaller emission linewidth (in single-frequency operation). A further reduction of the linewidth can be achieved by placing an intracavity filter such as the diffraction grating. Typical linewidths of an ECDL are below 1 MHz. One of these robust and reliable external cavity diode lasers is a model TA-Pro (Toptica) [24] hereafter as an L729.

2.1.1 The spectral characterisation of the L729 laser

The critical behaviour of the spectroscopy laser is the spectral linewidth below 1 Hz with the noise background at the level < 50 dB. In our case we use an external cavity diode lasers model TA-Pro (Toptica) [24] hereafter as an L729.

The first step is then to characterise the spectral properties of the L729. One traditional method for the laser spectral linewidth measurement is a beat-note measurement of the laser through optical mixing against a frequency-stable ultra-narrow linewidth laser. Unfortunately, in our case, we do not have another stable reference laser with l Hz linewidth at the non-traditional wavelength of 729 nm. However, we have an optical frequency comb FC1500 (Menlosystems GmbH) that generates the optical spectrum in the near-infrared part of the light spectrum with a doubling unit, so visible part of the spectrum can be reached. Based on this idea, I put together a setup where the L729 laser is optically mixed with the output of the optical frequency comb. As a dispersion element, the optical grating has been used as a filter to eliminate unwanted OFC's components before a fast photodiode. The resulted beat-note signal is shown in Fig. 2.1.

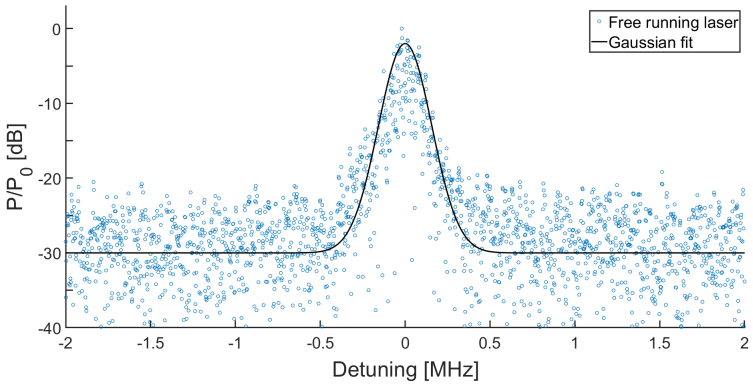

Figure 2.1: A spectral profile of the beat-note of a free running L729 and the optical frequency comb for the integration time 1 s. The laser spectral linewidth is 300 kHz approx..

The measurement shows that the spectral linewidth of beat-note is around 300 kHz approx for the integration time 1 s while our optical frequency comb has averaged tooth spectral linewidth about 50 kHz. It's clear that L729 contributes to the broad full-width at half maximum (FWHM) of the linewidth and thus it does not fulfil the requirement for the efficient pumping of long-lived forbidden transition ($S_{1/2}$ to $D_{5/2}$) of $^{40}Ca^{+}$ ion. Therefore an implementation of the linewidth narrowing technique for the L729 is necessary. In the following chapter, I will describe several techniques I have used to achieve a laser with a narrow spectral line for high-resolution spectroscopy purposes.

3. Emission line narrowing techniques

The basis of the laser system for high-resolution spectroscopy of Ca^+ cooled ions is the L729, whose spectral line-width is around 300 kHz. Therefore, this laser needs improvement with a technique that reliably ensures the direction of narrowing the broad spectral lines to the 1 Hz level. I have focused on several methods which I theoretically designed and experimentally implemented in my work. The main focused methods are:

- the technique of phase-locking the optical frequency of the laser on a selected tooth of an optical frequency comb,
- narrowing the broad spectral line-width with the help of a fibre interferometer,
- lock the optical frequency of the laser on a selected mode of a high-quality optical cavity,
- transferring the stability from ultra stable source using the transfer oscillator technique.

Following section is , I evaluated and compared the results achieved for the individually mentioned methods.

3.1 Phase lock to optical frequency comb

A phase-locked loop is a feedback system combining a tunable oscillator (the L729 in our case) and a phase comparator, which is usually implemented using an RF mixer. On a photodetector, the input laser is non-linearly mixed with a OFC tooth producing an RF beat note signal. Any changes in the input laser frequency will appear as a change in the phase of this beat note signal. The beat note signal phase is compared to that of an RF reference signal derived from the H-maser. This detected phase shift serves as an error signal for a cascade of fast and slow PID controllers actuating the laser optical frequency. In the equilibrium state of this control loop, the offset between the laser optical frequency and the nearest comb tooth will be locked to the frequency of the RF reference signal. Provided the bandwidth of the control loop is much higher than the original laser linewidth, the resulting spectral profile of the 729 nm laser will copy that of the selected optical frequency OFC tooth. The pilot testing setup of the scheme has been performed and can be seen in Fig. 3.1.

The advantage of this method, besides the line width narrowing, is that the L729 optical frequency is derived from a metrologically traceable time scale thanks to the referencing of the OFC with an active hydrogen maser that can reach a 10^{-15} fractional frequency stability for 10^4 s integration time. For high-resolution spectroscopy, this narrowing factor is still not sufficient. However, it is abundantly used for the rest of the wavelengths that do not require such a pure spectrum profile.

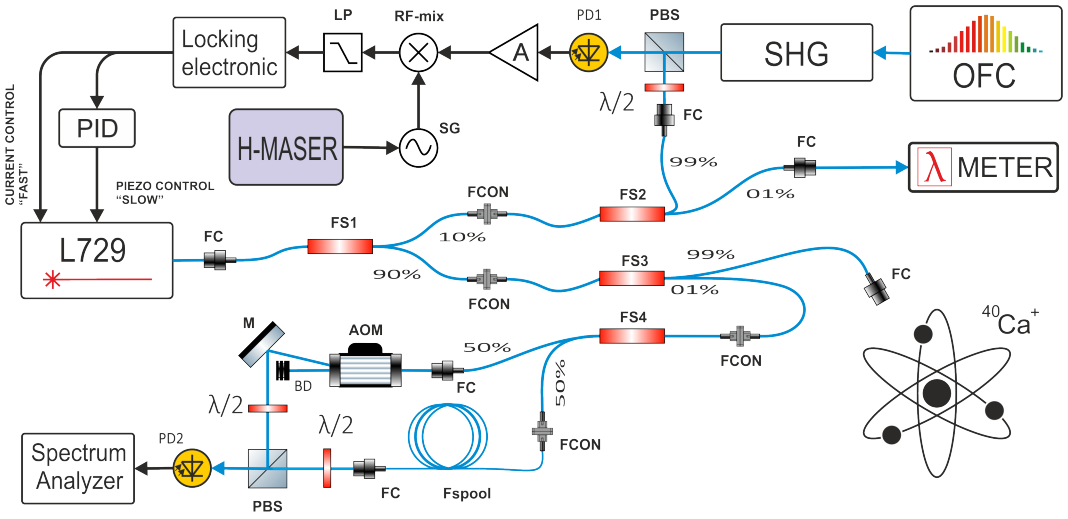

Figure 3.1: The setup with L729 laser and the phase lock loop chain for locking the optical frequency of the L729 laser to the optical frequency comb. LP: Low-pass filter, RF-mix: Radio frequency mixer, A: Amplifier, PID: Proportional Integral Derivative controller, SG: Signal generator, PD: Photodetector, PBD: Polarizing beamsplitter, FC: Fibre collimator, FS: Fibre splitter/coupler, FCON: Fibre connection, M: Mirror, BD: beam dumper, AOM: Acousto-Optic Modulator, $\lambda/2$: Half-wave plate, Fspool: Fibre spool, SHG: Second Harmonic Generation, H-maser: Hydrogen maser.

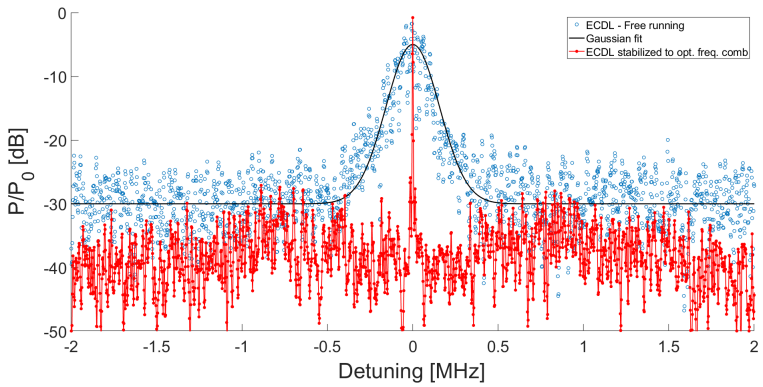

Figure 3.2: Normalized beatnote spectrum of the L729 laser. Comparison of free-running (blue) and stabilized to optical frequency Comb (red) regime.

3.2 Stabilization using fibre-spool

The fibre spool can work as a frequency discriminator. Thus one can use it also to spectral narrowing of the laser frequency. The fiber spool is built using a 500 m long single-mode fibre tightly wound in a helix form and gives a fixed relative time delay $\tau = 2.45$ μs. MZI then converts the deviation of the laser optical frequency (ν_{opt}) into phase error (φ_{err}) in the radio frequency domain.

The deviation of 1 Hz from the reference frequency in the optical domain will transfer into an approximately 15 μrad phase signal in the RF domain. If the fibre length is 5000 m, a 1 Hz deviation will convert into 150 μrad, etc. Here one can see that the sensitivity of the frequency discriminator is directly proportional to the length of the fibre spool.

I put together a setup where L729 linewidth is suppressed by MZI technique. The schematic diagram us shown in Fig. 3.3.In my experiment, the initial optical wave is divided into two separated waves by a 50/50 coupler. One enters the 500 m fibre spool, and the other one is frequency shifted by the AOM that is driven by an RF frequency f_{carr} = 80 MHz. A 50/50 beam splitter then recombines those two waves. This beat-note signal at a carrier frequency carries information about laser frequency noise and environmentally induced phase noise.

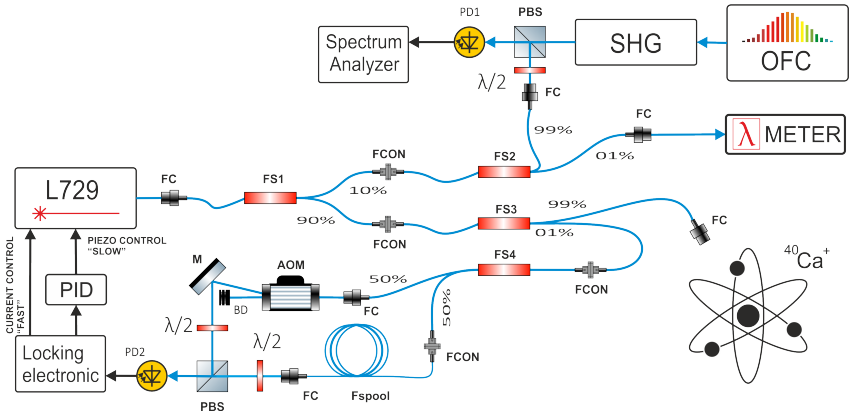

Figure 3.3: The schematic diagram of the stabilisation stage using Mach-Zehnder interferometer in the servo-loop. PID: Proportional Integral Derivative controller, PD: Photodetector, PBD: Polarizing beamsplitter, FC: Fibre collimator, FS: Fibre splotter/coupler, FCON: Fibre connection, M: Mirror, BD: beam dumper, AOM: Acousto-Optic Modulator, $\lambda/2$: Half-wave plate, Fspool: Fibre spool, SHG: Second Harmonic Generation.

I tested the L729 narrowed by MZI technique in the spectroscopy on the $S_{1/2} \rightarrow D_{5/2}$ transition on the single cooled calcium ion. Thus using the primary pulse sequence, including the electron shelving technique, the spectrum of one Zeeman component is obtained (see Fig. 3.4). We can see the carrier of this transition and its secular motional sidebands when the laser was scanned over the spectrum. The spectral linewidth of the laser stabilized by MZI technique is still very broad (<50 kHz).

3.3 Transfer oscillator technique

Another stabilisation method is based on using a so-called transfer oscillator technique described in [25, 26]. It allows us to transfer spectral profile of s highly coherent laser from one wavelength to another laser working at a different wavelength. In our case the

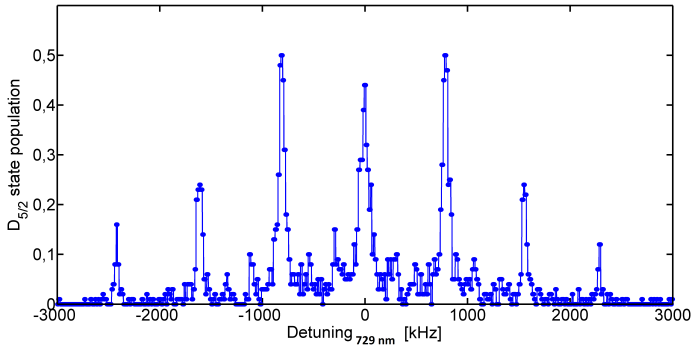

Figure 3.4: The captured spectrum of the the $S_{1/2} \rightarrow D_{5/2}$ transition of $^{40}Ca^{+}$ ion measured with the L729 narrowed by means of the unbalanced fibre-spool Mach-Zehnder interferometer.

reference is a laser working at 1540.57 nm (L1540) in our department at ISI CAS [27]. The laser L1540 is based on a narrow-linewidth fibre laser Basik1[1], which is phase locked to high-finesse optical cavity. This laser is used for stabilization of the optical frequency comb repetition frequency. Thanks to advanced synchronization technique where H-maser plays a role of disciplining oscillator for the OFC, the laser frequency of the L1540 is stable with the same relative stability as H-maser. I put together a pilot setup where the spectral profile and stability of the L1540 is transferred to spectroscopy L729 with using the OFC.

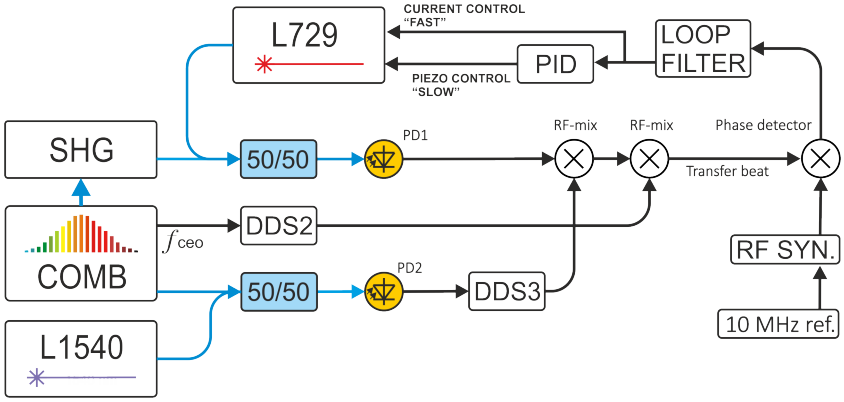

Figure 3.5: Transfer oscillator technique. DDS: Direct Digital Synthesizer, x/y: Fiber Optic Coupler. RF-mix: Radiofrequency mixer, PD: Photodetector. RF SYN: Radiofrequency synthesizer, 10 MHz reference is provide by hydrogen maser

The disadvantage of the transfer oscillator technique lies in the complexity of the whole setup with many broadband servo loops that inevitably lead to transferring residual noise from various sources, including complex locking electronics, into the resulting laser. Those

[1]NKT Koheras Basik.

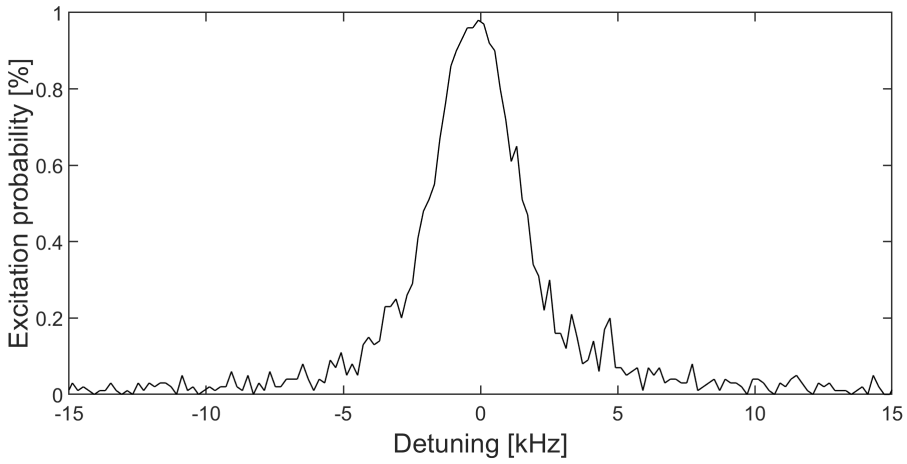

Figure 3.6: Frequency scan over a carrier on a transition $\Delta m = 0$ with a L729 narrowed by a Transfer oscillator technique, The spectral linewidth is 3 kHz approx.

residual noises interact with the ion in the form of off-resonance excitation of the transition lines, which reduces the fidelity and degrade the cooling process.

3.4 High finesse optical cavity at 729 nm

A more traditional and, so far, the most implemented method is the phase locking technique based on ultra-stable Fabry-Perot interferometers (FPI), also known as high-finesse (HF) cavities [28]. The optical cavity consists of two highly reflective mirrors optically contacted to stable spacer [29, 30]. The spacer is made from material that has a very low expansion coefficient, like Ultra-low Expansion glass (ULE®) or a silicon single-crystal [28, 31]. HF-cavities as references are broadly used and already commercialised (Stable Laser Systems)[32]. The important property of these cavities is that their fractional frequency instability of the longitudinal cavity mode directly relates to its fractional length instability. HF cavities can serve as very sensitive frequency discriminators. Using the Pound Drever Hall (PDH) [33] detection technique in a servo loop, we can lock a spectroscopy laser wavelength to the HF-cavity length and achieve the laser with Hz or sub-Hz spectral line width [31].

Moreover, one can find a relation between the finesse of the optical cavity and the locking process as the higher the finesse, the higher gain one can achieve in the control loop.

The limitation of this technique lies in two aspects. The first is an aging of the optical cavity's spacer which leads to permanent shift of the resonant frequency, thus very low frequency noise. The other aspect is in the Brownian thermo-mechanical noise [34, 35] in the material of mirrors, which directly leads to fluctuations of the optical length of the optical cavity and thus affects the frequency noise of the laser locked to it in

broad range of frequencies. Using this method for the spectroscopy laser narrowing and frequency stabilisation, the fractional frequency stability of the laser can reach 10^{-16} level for integration times shorter than 1 s.[4].

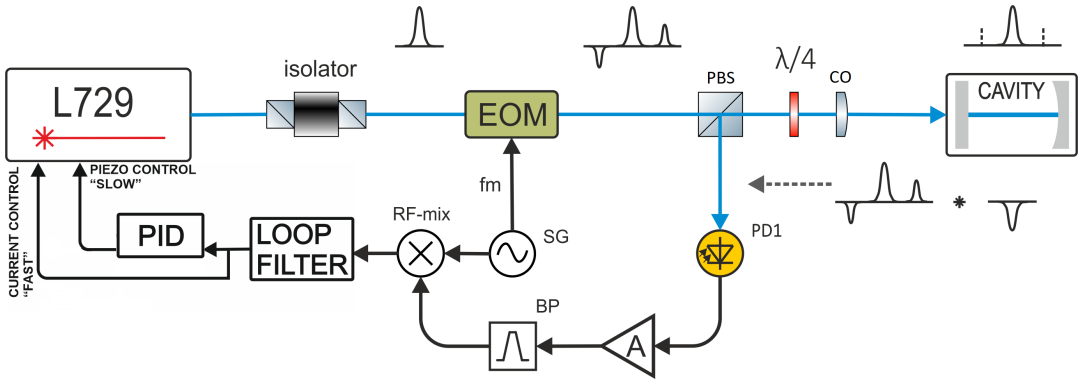

Figure 3.7: Scheme of the PDH locking technique. Isolator: Faraday islolator, EOM: Electro-optic modulator, PBS: Polarizin beamsplitter, SG: Signal generator, BP: Band-pass filter, A: Amplifier, CO: Collimation optics, PID: Proportional Integral Derivative controller, fm: modulation frequency.

The Fig. 3.7, shows the basic setup for PDH locking technique. The laser beam from the L729 is firstly sent through an optical isolator to avoid the back reflection of the laser to the laser diode. The laser beam is then phase modulated EOM and coupled into the optical cavity via the polarising beam-splitter and the quarter-waveplate. The reflected beam from the optical cavity is sent back through the quarter-waveplate and the beam-splitter into the avalanche photodetector.

4. Experimental setup

After a thorough investigation and implementation of various frequency stabilisation techniques, I considered the limitations of each technique. The result of implementation concludes that the best technique (in both short-term and long-term points) is to optically stabilise the L729 by locking its frequency to the ultra-stable HF-cavity (ULE C729) and providing additional control for keeping the aging effect of the C729 spacer at a very low level.

4.1 Optical setup

This section aims to present my final optical assembly that is currently used at the Institute of Scientific Instruments - ion setup. The assembly is used 24/7 for high spectroscopy on trapped and laser-cooled calcium ions for carrying out many experiments from metrology, quantum optics and mechanics. I carefully selected the best aspects out of all the methods described in the Subsec. 3 and embedded them in one single optical setup. The scheme of the whole optical setup is shown in the Fig. 4.1.

The setup can be divided into two main blocks. One with the implemented C729 and its optical requirement for the locking process. The second one is for producing the Ttransfer beat signal, which compensates for the C729 drift. A small portion of the light is firstly coupled and transported to the wavelength meter and the beating stage with the OFC. The main laser beam enters the setup with a single pass AOM for intensity stabilisation. The rest of the optical setup in the vicinity of the L729 is for frequency preparation before entering the chamber with cold $^{40}Ca^{+}$ ion.

4.1.1 Diode laser and fibres

The laser used for the experiment (L729) is a model TA-Pro[1]. TA-Pro series consists of a laser diode chip with one end being anti-reflection coated. The laser cavity is completed with a collimation lens and a mirror. This External-cavity diode laser is equipped with a tape amplifier (TA) which allows for high power (400 mW) at a wavelength of 729 nm. An intracavity diffraction grating provides a sufficiently wide coarse tuning of several nm. The correctly set laser typically provides approx. 20 GHz mode-hop free tuning range.

The fibre itself induces the noise into the laser light by Doppler effect. Thus the connection path with C729 is equipped with fiber cancellation (FNC). In the future, we plan to integrate this technique also on the rest of the long fibre connection.

[1]TA-Pro, Toptica, Germany [24].

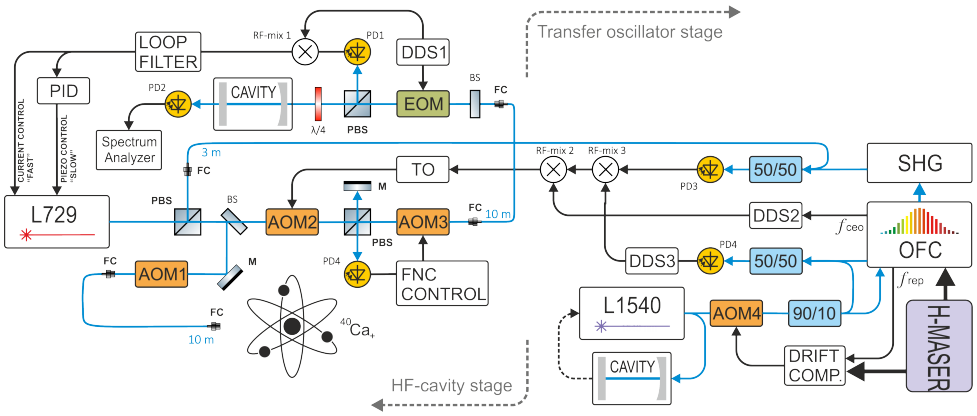

Figure 4.1: Setup for the frequency stabilization of the L729. PID: Proportional-Integral-Derivative controller, DDS: Direct Digital Synthesizer, Drift comp.: L1540 cavity drift compensation controller, AOM: Acousto-Optic Modulator, TO: Tracking oscillator, EOM: Electro-Optic Modulator, SHG: Second Harmonic Generation, FNC: Fiber Noise Cancelation, x/y: Fiber Optic Coupler.

Figure 4.2: Scheme of the TA-Pro (L729) [24]. The laser diode generate a stable light. After it pass the first isolator a portion of its light is steered out from the housing. This additional beam can be used for monitoring. The main wave is then amplified, passed through a second isolator and leave the laser housing. If the laser is well set, we can achieve an optical power of 400 mW°approx..

4.1.2 Optical frequency comb

In our laboratory, we use a commercially available frequency comb[2] with an intracavity electro-optic modulator based on an Er^{3+}-doped fibre oscillator with a repetition rate f_{rep} = 250 MHz. The offset frequency of the COMB f_{CEO} is locked to RF reference derived from a H-maser[3]. To get a broader range of optical frequencies, the output laser beam of the OFC is doubled by a second harmonic generation (SHG) process and broadened

[2]Menlo Systems M-Comb 1550.
[3]T4 Science iMaser 3000.

by a photonic crystal fibre to generate a super-continuum (broad optical spectrum). The result is the OFC spectrum range from 600 to 900 nm. This gives us a reliable instrument to stabilise all the wavelengths involved with $^{40}Ca^{+}$ (see Fig. 1.2).

4.1.3 Transfer oscillator technique

The transfer oscillator technique produces a virtual transfer beat-note between the L729 and the L1540[4]. The mediator between two lasers is the OFC. To achieve higher coherence of the L1540, it is locked to the c1540[5].

As it was described in Sec. 3.3, using special signal conditioning under "transfer oscillator technique", the frequency noise induced by f_{rep} and f_{ceo} is removed from the beat note between L729 and the nearest OFC tooth.

The resulting virtual beat note signal between L729 and L1540 can be used either for locking the L729 optical frequency directly to L1540 or for precise monitoring and compensation of drifting exhibited by the L729 locked to a C729. In the case of this work, the second approach brings more advantages since it leads to less high-frequency technical noise to the resulting laser spectral profile.

4.1.4 Acousto-optic modulators for spectroscopy purposes

In general, the laser frequency of the transition $S_{1/2} \leftrightarrow D_{5/2}$ of Ca^{+} does not coincide with the C729 resonance frequency. In our case, the laser frequency of L729 is needed to be tuned so that it matches the mentioned transition of the ion. For this purposes I used four AOMs[6]. They are used mainly for frequency shifting, intensity stabilisation and fibre noise cancellation.

4.1.5 Electro-optic modulators

The light leaving the collimator in the C729 side first passes through a Faraday isolator. This ensures that the light reflected back will not pass through the Faraday isolator again and will not be collimated back to the L729. It prevents unwanted lasing of L729 due to back-reflections from the optical setup. After that the light is phase modulated by an EOM[7] with frequency of $\omega = 12.9$ MHz producing the sidebands on the frequencies $\pm\Omega$ as seen in Fig. 4.3. The ratio of the optical power in the carrier and in the first sideband can be expressed as

$$\frac{P_{sideband}}{P_{carrier}} \approx 0.65. \tag{4.1}$$

[4]NKT Koheras Basik, working at 1540.57 nm.
[5]HF-cavity (ULE), Stable lasers, finesse approx. 4.5 x 10^5.
[6]Brimrose corp [36].
[7]Conoptic, model: 370 (USA)

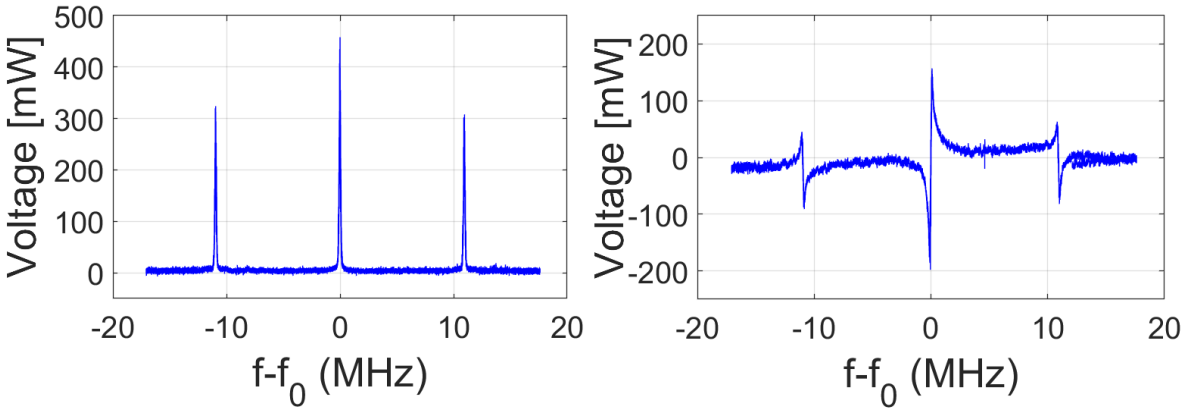

Figure 4.3: Frequency spectrum of the EOM output with carrier and the two first order sidebands, when modulating the laser light with $\omega = 12.9$ MHz (left). A corresponding PDH error signal as the frequency of the laser were scanned. The set-point for locking the laser frequency is in the middle of the slope of of this signal (right).

4.1.6 High finesse cavity

The HF-cavity C729 operated in our laboratory is a commercially available HF-cavity working at 729 nm purchased by Stable Laser Systems[8]. The high reflected coating on the mirror was fabricated by Advanced Thin Films. It consists of two fused silica mirrors of 0.165" thickness and 0.5" diameter, separated by a distance of 47.65 mm.

The C729 spacer to which the mirrors are attached is made from premium-grade ULE glass. This type of glass has a very low thermal expansion coefficient (typically $10^{-9}K^{-1}$

The fundamental cavity modes are separated by a $FSR = 3.14$ GHz. which correspond to a C729 lenth $= L = 47.65$ mm. The finesse of the C729 was determined by the decay time τ of the light field leaking out of the C729 during the ring-down response. The exponential fit to measured data yields an average photon storage time $\tau = 17.8\ \mu s$ thus, the finesse of C729 is quantified as 351 000 approx., and the corresponding linewidth of the fundamental cavity mode is $FWHM = 8.9$ kHz approx. This narrow transition provides enough room for detecting laser frequency changes down to a Hz level.

4.1.7 Optics for C729 incoupling and detection

After the EOM, the light passes through several optical components, namely the focusing lens, a beam sampler, a half-wave plate, a polarisation beam splitter (PBS) cube and the quarter-wave plate (in this order) until it reaches the first mirror of the C729. One needs to satisfy certain conditions for successful mode matching of the laser light into the resonance mode of the C729. The beam must be focused on the first mirror, the plane-parallel mirror. The beam waist at the position of this mirror has to have an appropriate

[8]Designed by D. R. Leibrandt et al. [30].

width. By taking in consideration the C729 diameter, the waist spot size on the PPM was determined to be 369 μm.

The quarter-wave plate ensures that the reflecting wave from the C729, which effectively passes the plate twice and thus has an opposite polarisation compared to the incoming light, will be redirected on PBS and focused into a fast photodetector. On the other side of the C729, the transmitted light is either detected by a sensitive photodetector[9], or it is redirected to the CCD camera[10] by a flip mirror.

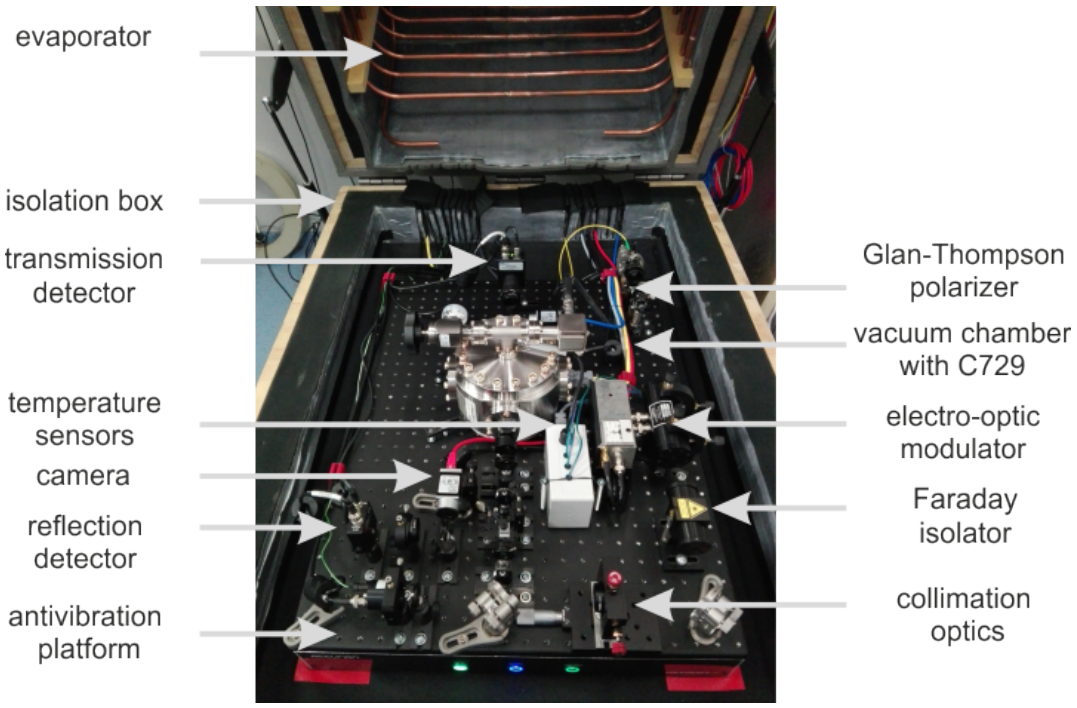

Figure 4.4: The optical setup for a mode-matching the laser wave into the C729. The vacuum chamber with the C729 is situated in the middle, surrounded by necessary optical and electro-optical elements for mode-matching, adjusting the beam waist and its spatial adjustment, cavity mode detection and generating the error locking signal. The temperature is measured at four points. Three PT100 temperature sensors are placed on the vacuum chamber and his surroundings. The one sensor provided by Stable Systems is place in close proximity of the C729. The temperature inside the box is regulated through a water circulating in the evaporator copper tube that is installed on the box walls.

4.2 Mechanical setup

The mechanical part of the setup consists of a vacuum chamber, where the HF-cavity C729 is placed. The whole idea is to provide the cavity with a stable operating conditions and isolate the cavity from environmental perturbations such as acoustic vibration and

[9]PDA-430A, variable-gain avalanche detector, Thorlabs.
[10]Basler Ace ac460.

temperature noises. The whole setup with individual isolation aspects can be seen in Fig. 4.5.

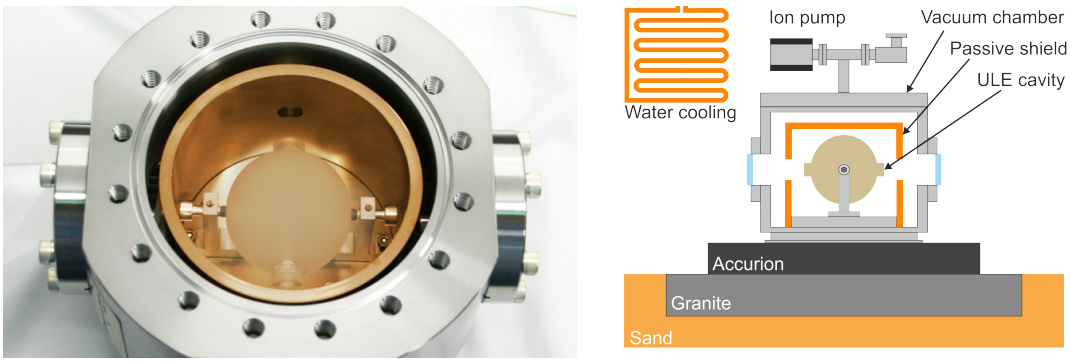

Figure 4.5: The view of the high-finesse optical cavity assembled in a vacuum chamber (left). Schematic of the vibration and thermal isolation platform, including the vacuum chamber and the gold, plated aluminium passive heat shield centred around the ULE cavity (The shield is temperature controlled with a Peltier element). The whole setup is then enclosed in a wooden box with thick layers of thermal isolation material (right).

4.2.1 Vacuum chamber for HF-cavity

To minimise the fluctuation of the refractive index of the inner part of the HF-cavity, environmental vibrations on the optical cavity and thus reach a low-level thermal noise, the C729 is sealed in the vacuum chamber[11]. A high-level vacuum inside the chamber is reached with the 3 l/s ion getter pump[12]. The pump provides stable pressure of 7.3 x 10^{-8}, which is enough to isolate the cavity from thermal convection and pressure fluctuation.

The chamber contains a Peltier element[13] and a thermistors with an impedance of 10 kΩ at 25 °C[14]. The thermistor is placed under the cavity holder and thus measures the temperature at very close proximity to the cavity. I used a PID-controler for temperature control of the cavity holder to keep the cavity on required temperature. The PID-controller for temperature control of the cavity holder to keep the cavitz on the required temperature. The PID-controller regulates the Peltier control current so that the temperature of the cavitz holder is in 1 mK stability range at the temperature 13.5 °C. Furthermore, the cavity is enclosed inside the gold-coated aluminium passive heat shield centred around the cavity. This shield prevents the temperature exchange via radiation between the cavity and chamber walls.

To prevent the temperature gradient between the laboratory environment and the vacuum chamber. The whole setup is enclosed into a 10 mm thick wooden box inside

[11]Thermally insulated Stainless Steel Vacuum VH630-Can, Stable laser systems.
[12]3S Titan Ion Pump, Gamma Vacuum.
[13]TE Technology HP-127-1.0-1.3-71R.
[14]General Electric MC65F103B.

coated with 76 mm thick foam made from compressed fibre glass[15] with 96 Kgm^{-3} density. This is the second temperature stabilizing stage. The temperature inside of the box is stabilised by a water cooling system made from copper pipes surrounding the box walls (the helical evaporator) (Fig. 4.5).

4.2.2 Vibration isolation and acoustic shielding

The vacuum chamber lies in the actively controlled vibration isolation table[16], with active bandwidth from 0.6 - 200 Hz. The isolation performance is min. 25 dB at 5 Hz and 40 dB at frequencies beyond 10 Hz. As the cavity is mounted the way that the axis of the spacer is horizontally oriented, I have decided to minimise the sensitivity of the spacers for vertical vibrations by placing the whole setup on a 250 kg block of granite. The granite block lies on a fine sand bed, and a thermal isolation box then encloses the whole setup. The block of sand is insulated from the floor by a rubber ELASTON-ELTEC FS 700 (GUMEX company) which is able to absorb mechanical energy between the floor and the sand block.

Acoustic insulation consists of a 1 cm thick wooden box, which serves as the first acoustic noise isolation. The inside of the wall is laid with 76 mm thick foam made from compressed fibre glass[17] with 96 Kgm^{-3} density suppressing noise from 100 Hz to 5 kHz. The followed 2 mm thick lead sheet also adds acoustic insulation.

4.2.3 Measurement of acoustic and vibration insulation

After completing the C729 arrangement, I provided measurement of the acoustic insulation of the wooden box by a vibrometer ABC123 placed on the Accurion table. There is visible very effective suppression of vibrations in the spectral range from 0.1Hz to 150Hz by a factor 20.

4.3 Electronic setup and digital control

All the electronics used for locking the L729 to the cavity and the electronics to produce the virtual transfer beat signal were designed and built by our electronics-engineering group in the ISI CAS. If possible, the care was taken to choose low-noise active components, especially operational amplifiers.

4.3.1 Active analog loop filter - controler

The active analog loop filter module plays a role of a fast controller for locking lasers by actuating their injection current with high frequency bandwidth and minimum transport

[15]Prima acoustic Broadband 3".
[16]Active vibration isolation system, Accurion halcyonics i4large M6/25.
[17]Prima acoustic Broadband 3".

delay. Basically, it is a cascade of three operational amplifiers. The first two stages act as integrators with limited frequency response. The third stage acts as a limited differentiator. The circuitry also contains buffer amplifiers for interfacing external instruments for monitoring the input and output signals.

4.3.2 Digital P-I-D controller

The digital P-I-D controller employs the NXP's 56F8365 16-bit digital signal controller to implement a medium-speed digital P-I-D controller for actuating the piezo tuning stages of the L729s. The input error signal is sampled using a 12-bit ADC with a 100 kHz sampling rate. The analog output control signal is produced by a 18-bit DAC at the same sampling rate.

4.3.3 Direct digital synthesizer

The direct digital synthesiser module is based on Analog Devices' AD9959 chip. This unit allows for simultaneously generating RF signals in 4 channels with coherent sampling. The frequency, relative phase and amplitude of each channel can be adjusted separately. The maximum generated frequency is 200 MHz. Using the on-chip PLL, the DDS sampling clock can be derived by multiplying a highly stable external reference signal. An 8-bit microcontroller (MCU) MC9S08DZ60 from NXP acts as an interface between the DDS chip and the CAN bus, which is used for the remote control.

4.3.4 Fibre noise cancellation controller

The fibre noise cancellation controller described more thoroughly in [27] is based on a modified printed circuit board of the original direct digital synthesiser module. The 8-bit MCU was replaced by a 32-bit high-speed STM32H753 digital signal processor (DSP) clocked at 400 MHz. The 16-bit ADC inputs of the DSP are digitising the output I and Q signals of an analog quadrature phase detector with the sampling rate of 4 MHz. Phase decoding and P-I-D control algorithms are implemented in the DSP that also steers the output frequency of the DDS chip over the SPI bus with 500 kHz sampling rate.

4.3.5 Digital control of the electronics and servo-loops

I used the electronics developed in ISI CAS for all control loops and supporting signal generation for providing the control of the optical setup in Fig. 4.4. I participated also on the LabVIEW software control algorithms and graphical interface for parametrization of the setup.

5. Experiments with trapped and laser cooled calcium ion

This chapter will deliver the measurement involving the spectroscopy laser. All the measurement involving the $^{40}Ca^{+}$ presented in this work were measured in the $|^2S_{1/2}, m = -1/2\rangle \leftrightarrow |^2D_{5/2}, m = -1/2\rangle$ transition ($\Delta m = 0$). This transition is least sensitive to magnetic fluctuation, so the measurement of frequency behavior of the laser L729 is the most accurate. When we have a stable and precise spectroscopy laser L729, we can perform many experiments with the calcium ion. All the related spectroscopic experiments on the $S_{1/2} \leftrightarrow D_{5/2}$ transition are carried out with electron shelving, thus in pulse sequence schemes. These schemes vary with the experiment but in general, are designed as the following (Fig. 5.1).

	t [ms]	866 nm	397 nm	397 nm sig.	854 nm	729 nm	APD	
1	1,000	■	■		■			Doopler cooling
2	0,200	■		■	■			State preparation
3	2,000	■			■	■		Sideband cooling
4	0,050	■		■	■			Clear out
5	0,005	■				■		Analysis
6	0,030	■						
7	3,000	■	■				■	Detection
8	0,010	■	■	■	■			Clear out

Figure 5.1: Typical pulse sequence scheme for interrogation of $S_{1/2} \leftrightarrow P_{1/2}$ transition in electron shelving regime. The scheme can be easily altered by adding more rows as the experiments require.

The description of the electron shelving steps:

- 1 - Doppler cooling: in the first step, the ion is Doppler cooled by probing the dipole $S_{1/2} \leftrightarrow P_{1/2}$ transition with a wavelength of 397 nm and 866 nm as a pumper. This results in the ion mean vibration quantum number of less than 10 (Doppler limit).
- 2 - State preparation: the state initialization step consists of wavelength 854 nm to prevent pumping into $D_{5/2}$ and an optical pumping into $|^2S_{1/2}, m = -1/2\rangle$
- 3 - Sideband cooling: this step requires the laser L729 to be frequency tuned into the lower motional sideband (the red sideband) of the ion secular motion. The motional ground state is achieved by applying a set of pulses at 729 nm accompanied by 854 nm. The 854 nm pulse repumps the population from long-live $D_{5/2}$ metastable state into a fast decaying $P_{3/2}$ state. After cooling pulses, the resulting mean

vibration quantum number is close to zero (typically 0.001). This motion state of the ion is called as a ground state.

- 4 - Clear out: to ensure that the for the following experiment, the entire population is actually at $S_{1/2}(m = -1/2)$ a short pulse of circularly polarised light (397 nm sig.) is applied to the $S_{1/2} \leftrightarrow P_{1/2}$ transition. A short pulse containing 854 nm for clearing the $D_{5/2}$ state is also included.

- 5 - Quantum state analysis: after the ion is prepared into its motional ground state by previously described steps, now we can perform a designed experiment by applying several pulses of light to the $D_{1/2} \leftrightarrow D_{5/2}$ transition. The pulse duration of this step varied with the different types of experiments.

- 6 - Waiting time: it is used for detection of the phase coherence between the laser L729 and the $D_{1/2} \leftrightarrow D_{5/2}$ transition.

- 7 - Detection: during the detection, the Doppler cooling lasers at 866 and 397 nm are switched on and the fluorescence is monitored for several milliseconds. By comparing the number of counts with a threshold value, we can discriminate whether the ion was at S or D level.

- 8 – Clear out: this is the final step of the electron shelving when the quantum state of the ion is ending at $S_{1/2}$ ground state.

5.1 Spectroscopy on Zeeman levels

With the pulse sequence mentioned above, I performed the spectroscopy on Zeeman components prepared by the magnetic field of ≈ 3.2 G influencing the cooled ion in the Paul trap. The π-pulse duration (see Fig. 5.1, line 5) and the power of the laser closely correlate to each other as one can transfer all population from S to D state either by shortening the pulse duration and at the same time increase the power. High power of the laser L729 can cause spectral power broadening. Thus, it is unsuitable for this measurement when a narrow line is required.

5.2 Rabi spectroscopy

Rabi spectroscopy is named after Isidor Isaac Rabi, who initially developed this method for measuring the particle frequencies of the two-level quantum mechanical systems. It is mainly used to analyze the cyclic behaviour of a two-level quantum system in the presence of the oscillating field. The Rabi spectroscopy consists of one interaction zone, where the ion interacts with the excitation laser. In the case of $^{40}Ca^{+}$ ion, the Rabi oscillation (or Rabi flop) is obtained by measuring the evolution of an excitation probability of the

$S_{1/2} \leftrightarrow D_{5/2}$ transition when the pulse duration τ of the laser L729 is scanned. The intensity of the spectroscopy laser is kept constant during the measurement.

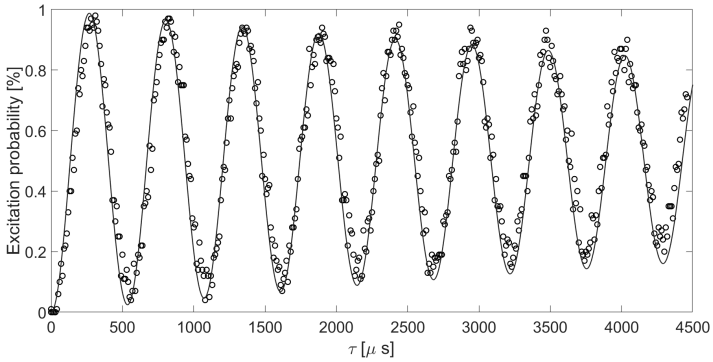

Figure 5.2: Rabi oscillation on the carrier of the $|^2S_{1/2}, m = -1/2\rangle \leftrightarrow |^2D_{5/2}, m = -1/2\rangle$ transition. If there are induced incoherence between the ground and excited levels, the Rabi oscillation slowly decays over the pulse length.

We can set the π-pulse to a certain time when we excite the $|S_{1/2}\rangle \leftrightarrow |D_{5/2}\rangle$ transition and scan the frequency over this transition. Thus the laser L729 is in scanning regime and We can see the carrier of the transition and motional sidebands generated by secular motion of the ion in the Paul trap.

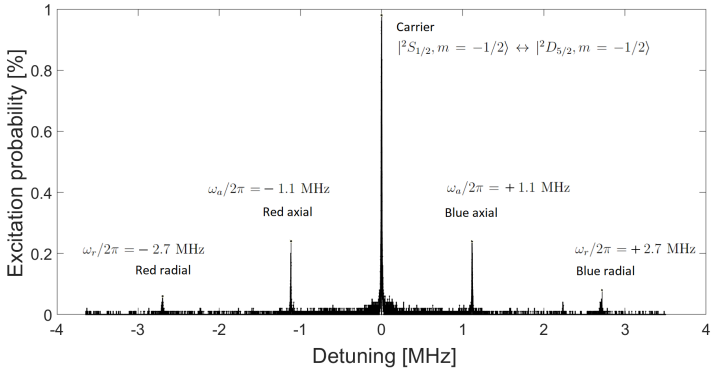

Figure 5.3: Spectrum of $|^2S_{1/2}, m = -1/2\rangle \leftrightarrow |^2D_{5/2}, m = -1/2\rangle$ transition measured with one ion in the trap. We see typical secular frequencies $\omega_r/2\pi = 2.7$ MHz in the radial and $\omega_a/2\pi = 1.1$ MHz in the axial direction.

Fig. 5.3 shows the frequency spectrum of one Zeeman component, more precisely $|^2S_{1/2}, m = -1/2\rangle \leftrightarrow |^2D_{5/2}, m = -1/2\rangle$ with its first axial and radial motional sidebands.

5.3 Ramsey spectroscopy

Ramsey spectroscopy, also known as a separated oscillating field method [37, 38], is a particle interferometry method used for measuring the particle transition frequencies. Today's

most precision atomic measurements, the SI unit definition of the second or atom interferometer, have a Ramsey-type configuration in detection chain.

The main goal of precision spectroscopy is to find the absorption frequency between the ground and the excited state of the ion. This can be accomplished by applying the external electromagnetic field at the frequency ω and finding the differences (also known as detuning Δ) between ω and the resonant frequency ω_0 of the transition. The excitation probability is maximized when $\Delta = 0$.

The Ramsey time determines the linewidth of the Ramsey fringe and thus the resolution with which Δ can be determined. The linewidth of the Ramsey fringe δ_ν is defined as $\delta_\nu \sim \frac{1}{\tau_R}$.

By increasing the τ_R one can increase the precision of the detected frequency detuning. The Ramsey fringe, as it is observed through the frequency scan, is shown in the Fig.5.4. The set parameters are $\pi/2$-pulses $= 20$ μs and Ramsey waiting time $\tau_R = 1$ ms. The Ramsey pattern is effectively an oscillation under the envelope of the Rabi method.

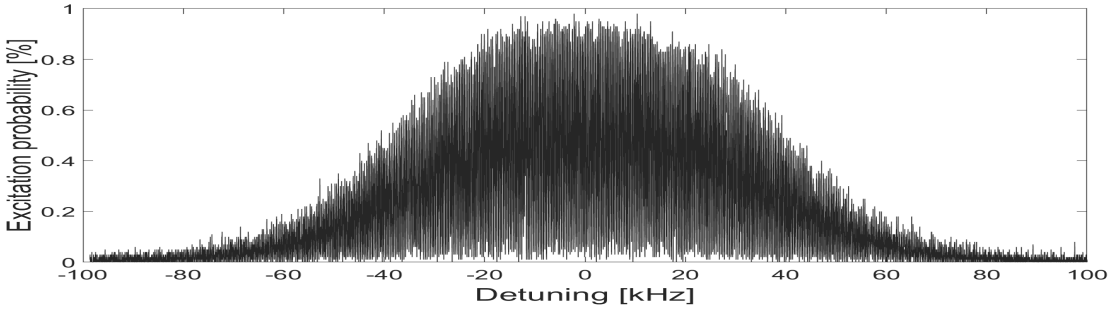

(a) Frequency scan over the carrier with Ramsey sequence.

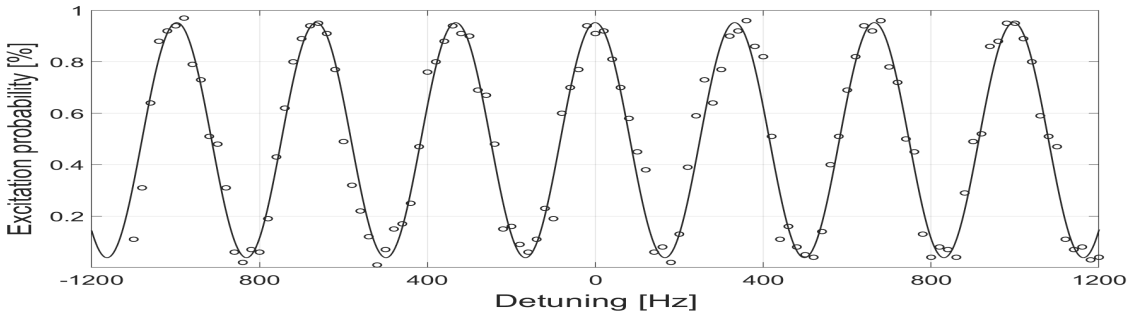

(b) A detailed zoom in 2 kHz window around the center frequency.

Figure 5.4: Frequency scan over the carrier of the $|^2S_{1/2}, m = -1/2\rangle \leftrightarrow |^2D_{5/2}, m = -1/2\rangle$ transition with a Ramsey sequence. The sequence consists of two $\pi/2$-pulses $= 20$ μs separated by Ramsey waiting time $\tau_R = 1$ ms.

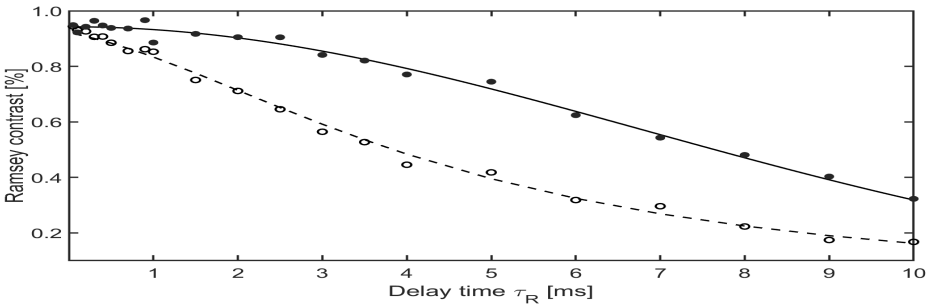

Figure 5.5: The contrast of the Ramsey pattern as a function of the delay time. Both (solid and open) circles are the data measured on the same Zeeman component ($|^2S_{1/2}, m = -1/2\rangle \leftrightarrow |^2D_{5/2}, m = -1/2\rangle$) with the same waiting time (τ_R). Open circles represented measurement when the L729 was locked to the virtual transfer beat. Solid circles represented the measurement when the L729 was referenced by HF-cavity length, and its drift was compensated using the transfer oscillator technique. The coherent time was extended nearly twice.

5.3.1 Test of qubit's decoherence

The Ramsey spectroscopy is perfectly suited for a test of qubit's decoherence [39]. The experiment consists of two $\pi/2$ pulses with a probe time duration of 20 μs separated by a waiting time τ_R. After applying the second pulse, the state of the ion is detected by electron shelving using the APD for fluorescence detection. Each experiment is repeated hundred times to obtain an excitation probability. Ideally, the excitation to $D_{5/2}$ should exhibit the modulation between zero and one when changing the phase between two pulses. The loss of contrast in this observed pattern is caused by a dephasing of the qubit levels when the superposition of the $|S\rangle$ and the $|D\rangle$ is exposed to decoherence for a long time, see Fig. 5.5.

The resulting laser linewidth $\Delta_{\nu_{FWHM}} = 29$ Hz corresponds to Ramsey time of 7.64 μs. Thus with L729 locked to C729 and using the TO as a fine-tuning tool, we increased the Ramsey contrast by order of two. For the comparison, I also measured the Ramsey contrast for $\Delta m = 2$ with a similar results.

5.3.2 Locking the L729 to $S_{1/2} - D_{5/2}$ transition

Ramsey spectroscopy is foremost used as a tool to reference the laser to the ion forbidden transition ($S_{1/2} \leftrightarrow D_{5/2}$).

To trace the frequency fluctuation of the laser and the resonance frequency of the transition I put two measuring point symmetrically at the slope around the center peak. I call them P_L and P_R (left and right side of the fringe).

P_L and P_R are separated by a line width of the fringe. We then set the frequency of the AOM f_{AOM} so that it matches the centre frequency f_{centre} of the highest peak. If the excitation probability at the f_{centre} changes due to a drop-off laser intensity, the

P_L and P_R will remain the same. When the excitation probability on the one measured point changes due to the frequency deviation from the f_{centre}, the excitation probability of the other measured point will change by the same amount but in the opposite direction. P_L and P_R are sent to the digital servo loop controller, which then accordingly adjusts the f_{AOM} so that the P_L and P_R are equal and ideally at 50% probability.

Usually, the clock stability is compared against a far more accurate reference. The most stable reference available in our laboratory in ISI CAS is H-maser. The stability of the H-maser can reach approx. 1×10^{-15} for the integration time in the vicinity of 10^4.

The ADEV in our case is computed from extracted frequencies f_{AOM} over the measured time. Here we can see that at the very short time τ, the ADEV is high. This is due to noise contribution. This hump at $\tau = 30$ s comes from the servo loop for compensating the drifting of c1540. This was later found during the comparison campaign between the ISI CAS and the Federal office of metrology and surveying [27]. At longer τ the noise is average out. Hence the ADEV decreases.

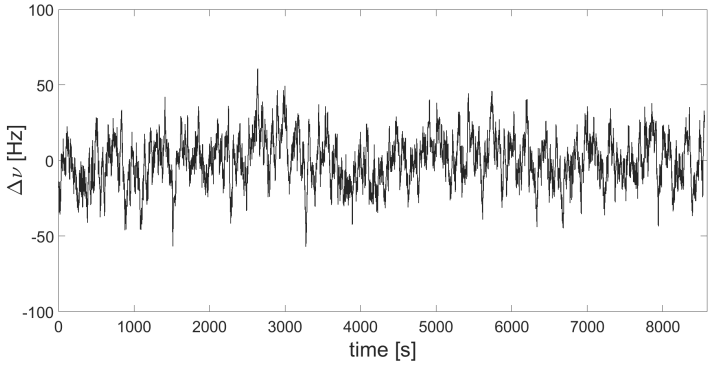

Figure 5.6: The extracted frequency deviation from the center frequency of $|^2S_{1/2}, m = -1/2\rangle \leftrightarrow |^2D_{5/2}, m = -1/2\rangle$ transition .

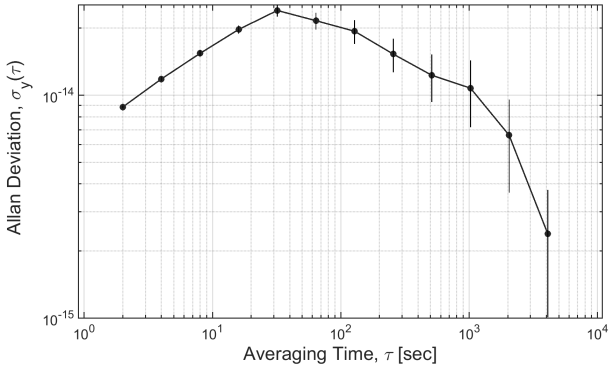

Figure 5.7: Allan deviation for extracted frequency of the AOM when L729 is locked to the $|^2S_{1/2}, m = -1/2\rangle \leftrightarrow |^2D_{5/2}, m = -1/2\rangle$ transition within Ramsey technique detection of the central frequency of this transition...

Conclusion

The heart of our optical atomic clock system is a $^{40}Ca^{+}$ ion. The clock transition of the Ca ion is an electric quadrupole transition $S_{1+2} \leftrightarrow D_{5/2}$. It has a rather long lifetime, > 1 s. Thus, to transfer the population into this level coherently, the probing laser has to have a linewidth at the Hz or sub-Hz level.

After a thorough investigation and implementation of various frequency spectral narrowing techniques, i.e. phase lock the laser to an optical frequency comb, stabilisation using the unbalanced Mach-Zehnder interferometer with a fibre spool, implementing a transfer oscillator technique. I came to the conclusion that the best technique (in both short-term and long-term point of view) is to optically reference the L729 by locking its optical frequency to the ultra-stable reference, a high finesse optical cavity followed de-drifting of the cavity aging by the complex setup with the optical frequency comb disciplined by the RF reference – Hydrogen maser. It led to very complex arrangement where I took many experiences from the field of vacuum technique, wave optics, polarization optics, optical modulators, spectroscopy detection techniques, control and analog and digital signal processing, RF electronics and finally as well as from the field of quantum physics and quantum mechanics.

I have designed and built a complete vacuum, optical and mechanical system to ensure reliable cavity operation. The optical part consists of elements for mode-matching the laser to the cavity and for generating the locking error signal. I designed and experimentally realized the mechanical arrangement of the cavity box witch isolated the cavity from the laboratory environment consisting of thermal fluctuation and vibration noise.

I put together the complex optical setup where the laser L729 optical frequency is locked to the cavity mode using the Pound-Drever-Hall detection technique in a servo loop. I implemented and fully exploited Ramsey spectroscopy technique for a test of qubit's decoherence of Ca^{+} ion with L729 laser and thus testing the performance of the spectroscopy laser. I have then systematically measured the Ramsey contrast for varied delay times between two pulses (5 s up to 10000 s)

The resulting laser linewidth of the L729 is $\Delta_{\nu_{FWHM}} = 29$ Hz witch corresponds to Ramsey time of 7.64 μs. I assume that the majority of the noise component causing the spectral broadening in the resulting laser linewidth is caused by the unstabilised optical fibre path between the laser and the vacuum chamber with the trapped ion. This will be a part of future research.

After my final adjustment of the narrowed laser L729 for spectroscopy purposes, the laser was used for many experiment in quantum physics, mechanics and time metrology. Since it was possible to achieve significant results with this laser, which were subsequently published (see Appendix I-III of the thesis), I consider the completed spectroscopic laser L729 to be the key to further research in the field of laser ion cooling, experiments in quantum mechanics and fundamental time metrology, such as the operation of an optical atomic clocks.

References

1. HALL, John L. Nobel Lecture: Defining and measuring optical frequencies. *Reviews of Modern Physics* [online]. 2006, vol. 78, no. 4, pp. 1279–1295 [visited on 2022-06-24]. Available from DOI: 10.1103/RevModPhys.78.1279. Publisher: American Physical Society.

2. HANSCH, Theodor W. Nobel Lecture: Passion for precision. *Reviews of Modern Physics* [online]. 2006, vol. 78, no. 4, pp. 1297–1309 [visited on 2022-06-24]. Available from DOI: 10.1103/RevModPhys.78.1297. Publisher: American Physical Society.

3. WINELAND, David J. Nobel Lecture: Superposition, entanglement, and raising Schrodinger's cat. *Reviews of Modern Physics* [online]. 2013, vol. 85, no. 3, pp. 1103–1114 [visited on 2022-06-24]. Available from DOI: 10.1103/RevModPhys.85.1103. Publisher: American Physical Society.

4. SCHIOPPO, M.; BROWN, R. C.; MCGREW, W. F.; HINKLEY, N.; FASANO, R. J.; BELOY, K.; YOON, T. H.; MILANI, G.; NICOLODI, D.; SHERMAN, J. A.; PHILLIPS, N. B.; OATES, C. W.; LUDLOW, A. D. Ultrastable optical clock with two cold-atom ensembles. *Nature Photonics* [online]. 2017, vol. 11, no. 1, pp. 48–52 [visited on 2022-06-24]. ISSN 1749-4893. Available from DOI: 10.1038/nphoton.2016.231. Number: 1 Publisher: Nature Publishing Group.

5. UDEM, Th.; DIDDAMS, S. A.; VOGEL, K. R.; OATES, C. W.; CURTIS, E. A.; LEE, W. D.; ITANO, W. M.; DRULLINGER, R. E.; BERGQUIST, J. C.; HOLLBERG, L. Absolute Frequency Measurements of the Hg+and Ca Optical Clock Transitions with a Femtosecond Laser. *Physical Review Letters* [online]. 2001, vol. 86, no. 22, pp. 4996–4999 [visited on 2022-05-30]. Available from DOI: 10.1103/PhysRevLett.86.4996. Publisher: American Physical Society.

6. DELVA, Pacôme; LODEWYCK, Jérôme. *Atomic clocks: new prospects in metrology and geodesy* [online]. 2013-08 [visited on 2022-05-30]. Tech. rep., arXiv:1308.6766. arXiv. Available from DOI: 10.48550/arXiv.1308.6766. arXiv:1308.6766 [gr-qc, physics:physics] type: article.

7. *Optical Atomic Clocks* [online]. 2015 [visited on 2022-06-20]. Available from DOI: 10.48550/arXiv.1407.3493. Number: arXiv:1407.3493 arXiv:1407.3493 [physics].

8. *Nuclear clocks for testing fundamental physics* [online]. 2020 [visited on 2022-06-20]. Available from DOI: 10.48550/arXiv.2012.09304. Number: arXiv:2012.09304 arXiv:2012.09304 [nucl-ex, physics:physics, physics:quant-ph].

9. *Fundamental Physics with a State-of-the-Art Optical Clock in Space* [online]. 2021 [visited on 2022-06-20]. Available from DOI: 10.48550/arXiv.2112.10817. Number: arXiv:2112.10817 arXiv:2112.10817 [gr-qc, physics:physics].

10. *Evaluation of the performance of a 40Ca+ - 27Al+ optical clock* [online]. 2020 [visited on 2022-06-20]. Available from DOI: 10.48550/arXiv.2012.05496. Number: arXiv:2012.05496 arXiv:2012.05496 [physics].

11. AHARON, Nati; SPETHMANN, Nicolas; LEROUX, Ian D.; SCHMIDT, Piet O.; RETZKER, Alex. Robust optical clock transitions in trapped ions. *New Journal of Physics* [online]. 2019, vol. 21, no. 8, p. 083040 [visited on 2022-06-20]. ISSN 1367-2630. Available from DOI: 10.1088/1367-2630/ab3871. arXiv:1811.06732 [physics, physics:quant-ph].

12. CAO, Jian; ZHANG, Ping; SHANG, Junjuan; CUI, Kaifeng; YUAN, Jinbo; CHAO, Sijia; WANG, Shaomao; SHU, Hualin; HUANG, Xueren. A transportable 40Ca+ single-ion clock with 7.7x10^(-17) systematic uncertainty. *Applied Physics B* [online]. 2017, vol. 123, no. 4, p. 112 [visited on 2022-06-20]. ISSN 0946-2171, ISSN 1432-0649. Available from DOI: 10.1007/s00340-017-6671-5. arXiv:1607.03731 [physics].

13. OBSIL, P.; LESUNDAK, A.; PHAM, T.; LAKHMANSKIY, K.; PODHORA, L.; ORAL, M.; CIP, O.; SLODICKA, L. A room-temperature ion trapping apparatus with hydrogen partial pressure below 10^(-11) mBar. *Review of Scientific Instruments* [online]. 2019, vol. 90, no. 8, p. 083201 [visited on 2022-06-19]. ISSN 0034-6748, ISSN 1089-7623. Available from DOI: 10.1063/1.5104346. arXiv:1904.13242 [physics, physics:quant-ph].

14. XU, Xiao-Tian; WANG, Zong-Yao; JIAO, Rui-Heng; YI, Chang-Rui; SUN, Wei; CHEN, Shuai. Ultra-low noise magnetic field for quantum gases. *Review of Scientific Instruments* [online]. 2019, vol. 90, no. 5, p. 054708 [visited on 2022-06-20]. ISSN 0034-6748, ISSN 1089-7623. Available from DOI: 10.1063/1.5087957. arXiv:1904.11642 [physics, physics:quant-ph].

15. MERKEL, B.; THIRUMALAI, K.; TARLTON, J. E.; SCHÄFER, V. M.; BALLANCE, C. J.; HARTY, T. P.; LUCAS, D. M. Magnetic field stabilization system for atomic physics experiments. *Review of Scientific Instruments* [online]. 2019, vol. 90, no. 4, p. 044702 [visited on 2022-06-20]. ISSN 0034-6748, ISSN 1089-7623. Available from DOI: 10.1063/1.5080093. arXiv:1808.03310 [physics, physics:quant-ph].

16. HANLEY, R. K.; ALLCOCK, D. T. C.; HARTY, T. P.; SEPIOL, M. A.; LUCAS, D. M. Precision measurement of the 43Ca+nuclear magnetic moment. *Physical Review A* [online]. 2021, vol. 104, no. 5, p. 052804 [visited on 2022-06-20]. ISSN 2469-9926, ISSN 2469-9934. Available from DOI: 10.1103/PhysRevA.104.052804. arXiv:2105.10352 [nucl-ex, physics:physics, physics:quant-ph].

17. RUSTER, T.; SCHMIEGELOW, C. T.; KAUFMANN, H.; SCHMIDT KALER, F.; WARSCHBURGER, C.; POSCHINGER, U. G. A long lived Zeeman trapped-ion qubit. *Applied Physics B* [online]. 2016, vol. 122, no. 10, p. 254 [visited on 2022-06-20]. ISSN 0946-2171, ISSN 1432-0649. Available from DOI: 10.1007/s00340-016-6527-4. arXiv:1606.07220 [quant-ph].

18. SAHOO, B.; ISLAM, M.; DAS, B; CHAUDHURI, R.; MUKHERJEE, D. Lifetimes of the metastable D3/2,5/22 states in Ca+, Sr+, and Ba+. *Physical Review A*. 2006, p. 62504.

19. DEMTRODER, W. *Laser Spectroscopy* [online]. [N.d.] [visited on 2022-05-30]. Available from: `https://link.springer.com/book/10.1007/978-3-662-05155-9`.

20. *SOLSTIS TITAN | SolsTiS | M Squared* [online]. [N.d.] [visited on 2022-06-22]. Available from: `https://www.m2lasers.com/solstis-titan.html`.

21. SHANK, C. V.; IPPEN, E. P. Subpicosecond kilowatt pulses from a mode-locked cw dye laser. *Applied Physics Letters* [online]. 1974, vol. 24, no. 8, pp. 373–375 [visited on 2022-06-22]. ISSN 0003-6951. Available from DOI: `10.1063/1.1655222`. Publisher: American Institute of Physics.

22. VALDMANIS, J. A.; FORK, R. L.; GORDON, J. P. Generation of optical pulses as short as 27 femtoseconds directly from a laser balancing self-phase modulation, group-velocity dispersion, saturable absorption, and saturable gain. *Optics Letters* [online]. 1985, vol. 10, no. 3, pp. 131–133 [visited on 2022-06-22]. ISSN 1539-4794. Available from DOI: `10.1364/OL.10.000131`. Publisher: Optica Publishing Group.

23. LITTMAN, Michael G. Novel geometry for single-mode scanning of tunable lasers. *Optics Letters* [online]. 1981, vol. 6, no. 3, pp. 117–118 [visited on 2022-05-30]. ISSN 1539-4794. Available from DOI: `10.1364/OL.6.000117`. Publisher: Optica Publishing Group.

24. TOPTICA. *TA pro* [online]. [N.d.] [visited on 2022-06-03]. Available from: `https://www.toptica.com/products/tunable-diode-lasers/amplified-lasers/ta-pro`.

25. STENGER, Jorn; SCHNATZ, Harald; TAMM, Christian; TELLE, Harald R. Ultraprecise Measurement of Optical Frequency Ratios. *Physical Review Letters* [online]. 2002, vol. 88, no. 7, p. 073601 [visited on 2022-05-25]. ISSN 0031-9007, ISSN 1079-7114. Available from DOI: `10.1103/PhysRevLett.88.073601`.

26. TELLE, H.R.; LIPPHARDT, B.; STENGER, J. Kerr-lens, mode-locked lasers as transfer oscillators for optical frequency measurements. *Applied Physics B: Lasers and Optics* [online]. 2002, vol. 74, no. 1, pp. 1–6 [visited on 2022-05-25]. ISSN 0946-2171, ISSN 1432-0649. Available from DOI: `10.1007/s003400100735`.

27. CIZEK, Martin; PRAVDOVA, Lenka; MINH TUAN, Pham; LESUNDAK, Adam; HRABINA, Jan; LAZAR, Josef; PRONEBNER, Thomas; AEIKENS, Elke; PREMPER, Jorg; HAVLIS, Ondrej; VELC, Radek; SMOTLACHA, Vladimir; ALTMANNOVA, Lada; SCHUMM, Thorsten; VOJTECH, Josef; NIESSNER, Anton; CIP, Ondrej. Coherent fibre link for synchronization of delocalized atomic clocks. *Optics Express* [online]. 2022, vol. 30, no. 4, p. 5450 [visited on 2022-05-20]. ISSN 1094-4087. Available from DOI: `10.1364/OE.447498`.

28. YOUNG, B. C.; CRUZ, F. C.; ITANO, W. M.; BERGQUIST, J. C. Visible Lasers with Subhertz Linewidths. *Physical Review Letters* [online]. 1999, vol. 82, no. 19, pp. 3799–3802 [visited on 2022-05-20]. ISSN 0031-9007, ISSN 1079-7114. Available from DOI: 10.1103/PhysRevLett.82.3799.

29. STERR, U.; LEGERO, T.; KESSLER, T.; SCHNATZ, H.; GROSCHE, G.; TERRA, O.; RIEHLE, F. Ultrastable lasers: new developments and applications. In: IDO, Tetsuya; REID, Derryck T. (eds.) [online]. San Diego, CA, 2009, 74310A [visited on 2022-05-20]. Available from DOI: 10.1117/12.825217.

30. LEIBRANDT, David R.; THORPE, Michael J.; NOTCUTT, Mark; DRULLINGER, Robert E.; ROSENBAND, Till; BERGQUIST, James C. Spherical reference cavities for frequency stabilization of lasers in non-laboratory environments. *Optics Express* [online]. 2011, vol. 19, no. 4, p. 3471 [visited on 2022-05-20]. ISSN 1094-4087. Available from DOI: 10.1364/OE.19.003471.

31. ALNIS, J; MATVEEV, A; KOLACHEVSKY, N; WILKEN, T; UDEM, Th; HANSCH, T W. Sub-Hz line width diode lasers by stabilization to vibrationally and thermally compensated ULE Fabry- Perot cavities. [N.d.], p. 18.

32. STABLE. *Home* [online]. [N.d.] [visited on 2022-07-03]. Available from: https://stablelasers.com/.

33. DREVER, R. W. P.; HALL, J. L.; KOWALSKI, F. V.; HOUGH, J.; FORD, G. M.; MUNLEY, A. J.; WARD, H. Laser phase and frequency stabilization using an optical resonator. *Applied Physics B Photophysics and Laser Chemistry* [online]. 1983, vol. 31, no. 2, pp. 97–105 [visited on 2022-05-20]. ISSN 0721-7269, ISSN 1432-0649. Available from DOI: 10.1007/BF00702605.

34. KELLER, Jonas. Spectroscopic characterization of ion motion for an optical clock based on Coulomb crystals. [N.d.], p. 135.

35. NUMATA, Kenji; KEMERY, Amy; CAMP, Jordan. Thermal-Noise Limit in the Frequency Stabilization of Lasers with Rigid Cavities. *Physical Review Letters* [online]. 2004, vol. 93, no. 25, p. 250602 [visited on 2022-05-20]. ISSN 0031-9007, ISSN 1079-7114. Available from DOI: 10.1103/PhysRevLett.93.250602.

36. BRIMROSE. *Brimrose Corp.* [Online]. [N.d.] [visited on 2022-06-16]. Available from: https://www.brimrose.com.

37. RAMSEY, Norman F. A New Molecular Beam Resonance Method. *Physical Review* [online]. 1949, vol. 76, no. 7, pp. 996–996 [visited on 2022-05-20]. Available from DOI: 10.1103/PhysRev.76.996. Publisher: American Physical Society.

38. RAMSEY, Norman F. A Molecular Beam Resonance Method with Separated Oscillating Fields. *Physical Review* [online]. 1950, vol. 78, no. 6, pp. 695–699 [visited on 2022-06-27]. Available from DOI: 10.1103/PhysRev.78.695. Publisher: American Physical Society.

39. SCHMIDT-KALER, F; GULDE, S; RIEBE, M; DEUSCHLE, T; KREUTER, A; LANCASTER, G; BECHER, C; ESCHNER, J; H FFNER, H; BLATT, R. The coherence of qubits based on single Ca ions. *Journal of Physics B: Atomic, Molecular and Optical Physics* [online]. 2003, vol. 36, no. 3, pp. 623–636 [visited on 2022-05-20]. ISSN 0953-4075. Available from DOI: 10.1088/0953-4075/36/3/319.

Appendix I

Key publications and my contribution

Here is a list of the first- and co-authored publications included in the doctoral thesis, together with my contribution to each article.

- **Research article 1**

A room-temperature ion trapping apparatus with hydrogen partial pressure below 10^{-11} mBar

P. Obšil, A. Lešundák, T. Pham, K. Lakhmanskiy, L. Podhora, M. Oral, O. Číp, and L. Slodička
Review of Scientific Instruments (2019), DOI: 10.1063/1.5104346

Contribution:

- I participated in preparing, cleaning and assembly of vacuum apparatus.
- I participated in preparing and assembly of apparatus for loading and trapping ion.
- I prepared and build an optical path for ionisation lasers.
- I prepared and build an optical path for Doppler lasers.
- I prepared and build an optical path for spectroscopy laser.
- I participated in building an optical path for fluorescence detection.
- I controled and managed technical support during measurements.
- I prepared and participated in measurements.
- I participated in editing the manuscript.

- **Research article 2**

Optical frequency analysis on dark state of a single trapped ion

A. Lesundak, T. M. pham, M. Cizek, P. Obsil, L. Slodicka, and O. Cip
Optics Express (2020), DOI: 10.1364/OE.389411

Contribution:

- I controled and managed technical support during measurements.
- I prepared and build an optical path for Doppler lasers.
- I prepared and participated in measurements.
- I participated in processing the data.
- I participated in editing the manuscript.

- **Research article 3**

Frequency stabilisation of 729 nm external cavity diode laser with a combined approach using the high finesse cavity and transfer oscillator technique

---

M. T. Pham, M. Cizek, A. Lesundak, A. Kovalenko, P. Obsil, P. Jedlicka, L. Slodicka and O. Cip

Contribution:

- I cleaned and put together the vacuum setup for HF-cavity C729.
- I designed and put together an optical setup for locking the laser to HF-cavity.
- I put together isolation elements, designed and and build an insulation box.
- I designed and put together a water cooling system.
- I participated in cleaning and assembling a vacuum setup for HF-cavity c1540.
- I participated in assembling of optical setup for mode-matching the laser to HF-cavity.
- I designed and put together an optical path for Doppler lasers.
- I designed and build an electro-optical setup for spectroscopy laser.
- I designed and build an electro-optical setup for interation with the trapped ion.
- I designed and build an electro-optical setup for fiber noise cancelation.
- I designed the experiment with trapped and cooled ion, measured and analyzed the data.

Curriculum vitae

PERSONAL INFORMATION

Pham Minh Tuan

Královopolská 147, 612 64 Brno, Czech Republic

+420 541 514 532 +420 731 819 893

tuan@isibrno.cz

http://www.isibrno.cz/

Sex Male | Date of birth 05/05/1988 | Nationality Czech Republic / Viet Nam

WORK EXPERIENCE

2014-onwards

Ph.D. Student

Institute of Scientific Instruments, Czech Academy of Sciences, Královopolská 147, 612 64 Brno, Czech Republic

- Frequency stabilization of laser working at 729 nm for ion cooling.
- Research in laser optics and laser spectroscopy with trapped and cooled Ion.
- Vacuum technology, design and assembly of new apparatus.
- High finesse optical resonators and stabilisation techniques.

Science, optics, metrology

2012-onwards

Technologist of DBR diode lasers

Institute of Scientific Instruments, Czech Academy of Sciences, Královopolská 147, 612 64 Brno, Czech Republic

- Technology and investigation of broad tunable narrow-linewidth diode laser working at 633 nm for metrology and molecular spectroscopy.

Science, optics, metrology

EDUCATION AND TRAINING

2014-onwards

Doctoral study, Ph.D.

ISCED6

Brno University of Technology, Faculty of Mechanical Engineering, Institute of Physical Engineering, program Physical and Material Engineering

- Ph.D. Thesis: " Single-frequency laser with narrow spectral linewidth for cold ion spectroscopy"

2012-2014

Master study, Dipl.- Ing.

ISCED5

Brno University of Technology, Faculty of Electrical Engineering and Communication, Institute of Biomedical Engineering, study program Biomedical Engineering and Bioinformatics.

- Diploma thesis: "Analysis of volumetric change of hippocampus caused by Alzheimer's disease", a development of software for analysing and segmentation of 3D data from MRI.

05-06/2018

Visiting researcher"

The National Physical Laboratory, GB

- building and characterising an Yb+ ion trap for use in Host's optical atomic clock. Building an optical and electrical infrastructure for stabilising an optical frequency on high finesse cavity.

06/2017

Professional course "Time and Frequency seminar"

The National Institute of Standards and Technology, US

- optical clock, oscillators, atomic frequency standards, quantum information, phase-noise measurements

8/2016

Visiting researcher"

The Observatoire de Paris, France

- Frequency tripling of telecom laser diode
- Stabilisation of the lase to iodine hyperfine line

07/20016, 1 week

The 26th International Travelling Summer School on Microwaves and Lightwaves

L´Aquila, Italy

- Laser instrumentation, optics, terahertz technologies and application.

PERSONAL SKILLS

Mother tongue(s): Vietnamese

Other language(s):

	UNDERSTANDING		SPEAKING		WRITING
	Listening	Reading	Spoken interaction	Spoken production	
Czech	C2	C2	C1	C1	C1
English	B2	B2	B2	B2	B1

Communication skills: Ability to work and communicate in teams. Good communication adaptation due to many international visited work travels and conference in different fields of interest.

Organisational / managerial skills: Doctoral and high school studies and managerial skills gained through managing of investigated projects. Organisational and pedagogic skills gained through experiences from many years of leading sport and health related clubs.

Job-related skills: Experience gained through daily experimental laboratory work with optics and optomechanics. Design and realization of vacuum and optomechanical assembly. Collecting and processing measured data.

Computer skills: Routine usage of PC, office SW, Corel Draw, programming and processing of scientific data in MATLAB computational SW, programming and controlling of experiments in LabVIEW, Design of electronic circuits and printed circuit boards via system Eagle. Design of mechanical parts using Autodesk Inventor.

Driver licence: B

ADDITIONAL INFORMATION

Applied research results: Product:1
Software for segmentation and measuring of volume of hippocampus, 2014

Honours and awards: 2016 – Award of the ITSS (International Travel Summer School on Microwaves and Lightwaves) – First place for team project.

Abstrack

The thesis deals with stabilising a diode laser operating at a wavelength of 729 nm, which is used for high-resolution spectroscopy and interacting with captured and cooled calcium ions. Interaction with the ion requires an extremely narrow spectral linewidth for the excitation laser. The work explains essential procedures and methods leading to the operation of a laser with a spectral linewidth in the order of Hz or less. The central part of the work is to design and put together an optical assembly for this laser with the necessary electro-optical elements. The main emphasis is placed on laser frequency stabilisation techniques using external references, their theoretical description and implementation are also a part of this work. The first chosen approach to narrowing the spectral linewidth is locking the optical frequency of the laser to a selected component of the optical frequency comb using electronic phase locks. Spectral noise measurements were performed using a two-beam interferometer with unbalanced arms. The achieved noise suppression results for the locked laser were then compared with the free-running laser mode. Another approach is to lock the spectral line of the laser to a very narrow line of a high-quality optical resonator. With this method, I achieved a laser with a very narrow spectral line (in the order of tens of Hz), however, with short-term stability. The next step was the construction and use of the "transfer oscillator" technique, which provided additional compensation for the unwanted drift of the resonance mode of the optical resonator and thereby ensured the long-term stability of the entire system. The laser stabilised in this way at 729 nm was tested in spectroscopy on the forbidden transition of the Doppler-cooled calcium ion.